JOURNAL OF MASS SPECTROMETRY, VOL. 33, 45–54 (1998)

Gas-phase Dimerization of Dimethylaniline in an External Electrospray Fourier Transform Mass Spectrometer

E. Peter Maziarz, III, and Troy D. Wood*†
Department of Chemistry, Natural Sciences Complex, State University of New York at Buffalo, Buffalo, New York 14260-3000, USA

N*,*N*-Dimethylaniline (DMA) is a common starting material in graft copolymerization and photopolymerization processes when combined with an organic acid. Several anodic oxidation studies of DMA, in an acidic medium, have been performed. Numerous electrochemical studies imply that DMA has a tendency to dimerize, forming the tail-to-tail coupling product *N*,*N*,*N*′,*N*′-tetramethylbenzydine (TMB). Here, external electrospray ionization Fourier transform mass spectrometry was used to investigate the dimerization and charging characteristics of DMA in an acidic medium in the absence of an applied electrochemical technique. DMA forms both tail-to-tail and head-to-tail dimer products, and the different linkage types were determined by employing tandem mass spectrometry for structure elucidation. In addition, it was found that desolvated protonated DMA ions accumulated and stored in the hexapole ion guide for 1–10 s before transport to the trapped ion cell can undergo gas-phase ion–molecule reactions to form dimeric products, including doubly charged species. Hence the hexapole storage region can be used to conduct ion–molecule reactions away from the low-pressure ion trap. © 1998 John Wiley & Sons, Ltd.

J. Mass Spectrom. Vol. **33**, 45–54 (1998)

KEYWORDS: dimethylaniline; dimerization; electrospray ionization; tandem mass spectrometry; Fourier transform mass spectrometry

INTRODUCTION

N,*N*-Dimethylaniline (DMA) is a common starting material in graft copolymerization and photopolymerization processes when combined with an organic acid. For example, DMA is used as a starting material for the polymerization of vinyl monomers.[1] DMA coupled with copper (II) ion, in an acidic medium, has been shown to initiate graft copolymerization of methyl methacrylate onto natural rubber.[2] Ghosh and Chowdhury[3] showed that DMA is an effective photoinitiator for the photopolymerization of methyl methacrylate when combined with an organic acid. A common trend noted in the above investigations is that the acid medium effects the nature and utility of the final polymer product, and therefore plays an important role in the functionality of DMA. In another study, Oyama *et al.*[4] formed an ionene polymer of DMA from electrochemical synthesis in an acidic medium. The resulting product found utility as an anion-exchange film.

Historically, anodic oxidation studies of aromatic amines in acidic media have been investigated with the intention of understanding the mechanisms of electrochemically generated products *in situ*.[5–9] The chemistry of aromatic amine compounds is dominated by the lone electron pair on nitrogen leading to the formation of oligomeric and polymeric products.[10] Dimeric products of aromatic amines are often referred to as having head-to-tail (htt) or tail-to-tail linkages (ttt).[5,8,11] Dimeric products of aniline have served as simplified model systems for understanding and characterizing polyaniline.[12] The tendency for DMA to form the (ttt) dimer product *N*,*N*,*N*′,*N*′-tetramethylbenzydine (TMB) when subjected to electrochemical conditions is well known.[13–16] A number of possible mechanisms for TMB formation have been proposed involving electron transfer reactions, including those involving *para–para* and *ortho–para* ttt couplings.[13–16] Neubert and Prater[16] suggested a pseudo first-order net reaction for the formation of TMB in which dimerization occurs between neutral radicals. An interesting investigation using thermospray ionization mass spectrometry was evaluated as a tool to detect electrochemically generated products from solution with DMA as the model compound.[17] The investigators reported the formation

* Correspondence to: T. D. Wood, Department of Chemistry, Natural Sciences Complex, State University of New York at Buffalo, Buffalo, New York 14260-3000, USA. Email address: twood@acsu.buffalo.edu

† Also Department of Chemistry, Roswell Park Cancer Institute, Elm and Carlton Streets, Buffalo, New York 14263, USA.

Contract grant sponsor: Petroleum Research Fund.

Contract grant sponsor: State University of New York at Buffalo.

CCC 1076–5174/98/010045–10 $17.50

Received 18 June 1997
Accepted 25 September 1997

of TMB consistent with previously postulated mechanisms, in addition to evidence of the formation of DMA trimers.

Tandem mass spectrometry (MS/MS) is a technique well known for its power in elucidating ion structures.[18,19] Despite this, no studies employing MS/MS to investigate the structural nature of DMA 'dimers' in an acidic solution medium (in the absence of applied electrochemical means) proposed in the electrochemistry literature have been performed. Recently, electrospray ionization mass spectrometry (ESI-MS)[20] has emerged as a tool to study compounds that can be ionized in solution via Brønsted–Lowry or Lewis acid–base chemistry. Van Berkel *et al.*[21] have shown that aromatic amines can be analyzed via ESI in an acidic medium, whereby a nitrogen atom in the amino form is transformed into its quaternary ammonium form. It is well established that quaternary nitrogen compounds can be weakly electrophilic.[22] The dimethylamine group $[(CH_3)_2\ N]$ on neutral DMA is a strong electron donor, making it susceptible to attack from weak electrophiles.[23] These characteristics suggest the possibility that protonated DMA ($[DMAH]^+$) and DMA could combine in solution to form an ionene dimer.

Here, a commercial external electrospray ionization Fourier transform (FT) mass spectrometer employing a linearized Infinity cell[24] was used to investigate the dimerization and charging characteristics of DMA in an acidic solution. Tandem mass spectrometry was employed to help distinguish between htt and ttt dimeric products. Tandem ESI-FTMS reveals that in an acidic medium, DMA forms a variety of dimeric products encompassing structures with either htt or ttt linkages. In addition, prolonged storage in the hexapole ion guide in the external ESI source shows evidence of gas-phase reaction of monomeric $[DMAH]^+$ and DMA to form a variety of dimeric ion–molecule reaction product ions, suggesting a general utility of the hexapole ion guide for conducting high-pressure ion–molecule reaction experiments.

EXPERIMENTAL

ESI-FTMS instrumentation

All experiments were conducted on a Bruker (Billerica, MA, USA) BioApex 30es Fourier transform mass spectrometer equipped with an Analytica of Branford (Branford, CT) ESI source with an Iris hexapole ion guide. A similar ESI source has been illustrated and described previously by Lau *et al.*[25] The instrument design and a description of the 3.0 T magnet and pumping system used here have been reported elsewhere.[26] A Cole-Palmer (Vernon Hills, IL, USA) Series 74900 infusion pump was used to inject analyte samples continuously into the ESI source at a rate of 60 $\mu l\ h^{-1}$. Nitrogen countercurrent drying gas (290 °C) at a flow rate of 1–2 $l\ min^{-1}$ was used to desolvate droplets produced by the ESI source. A potential between −3.6 and −3.8 kV (relative to the grounded needle) was applied to the metal-capped glass capillary. Ions were injected into the Infinity cell,[24] having a 2.0 V trapping voltage, using the Sidekick method.[27] Frequency-sweep excitation from m/z 10 to 700 was applied at an amplitude of ~ 44–$63\ V_{pp}$. Detection was in the direct mode (500 kHz Nyquist bandwidth) from time domain data sets of 128K (ten scans per experiment). The data sets were apodized with a Gaussian function, Fourier transformed and displayed in magnitude mode. Zero-filling was not employed.

Tandem mass spectrometry

Parameters used in the tandem MS experiments varied and are given in the figure legends. In general, correlated sweep was used to isolate the ion of interest. A pulsed valve was used to admit argon gas (2×10^{-7}–7×10^{-7} mbar) into the analyzer trap prior to ion activation and dissociation by sustained off-resonance-induced collision-activated dissociation (SORI-CAD).[28]

Hexapole ion accumulation study

Desolvated ions were accumulated and stored in the hexapole ion guide for 1–10 s before transport to the trapped ion cell. A pressure of 10^{-3}–10^{-4} mbar was maintained in the hexapole region by an Edwards EXT250H turbomolecular pump. The ion storage time was controlled from Bruker's XMASS software on a Silicon Graphics (Mountain View, CA, USA) INDY 100 MHz R4600PC system operating with 32 MB RAM. All other parameters were held constant during these experiments to insure that the observed effects were due to the hexapole storage accumulation time.

Sample preparation

Reagent-grade DMA was obtained from J. T. Baker (Phillipsburg, NJ, USA) and used without further purification. All samples were initially prepared as ~ 3.0 mM DMA stock solutions in a solvent system composed of MeOH–H_2O–acetic acid (49:49:2, v/v/v). The pH of the stock solution was measured with a Hanna Instruments HI 1295 Piccolo plus pH meter and found to be 3.15 ± 0.05. HPLC-grade methanol and acetic acid were obtained from commercial suppliers and used without further purification. Sample solutions for ESI were prepared by serial dilution to produce $\sim 30\ \mu$M DMA for analysis.

RESULTS AND DISCUSSION

ESI-FTMS of DMA

The chemistry of DMA is dominated by the lone electron pair on nitrogen, accounting for its Brønsted–Lowry base behavior and its ability to form protonated DMA with the nitrogen in its quaternary ammonium form.[10,21] The pK_a values of DMA and acetic acid are 5.15 and 4.74, respectively, suggesting that protonated DMA ($[DMAH]^+$) can be formed in solutions containing acetic acid. Figure 1 shows a mass spectrum of 30 μM DMA in ESI solution $[DMAH]^+$ is

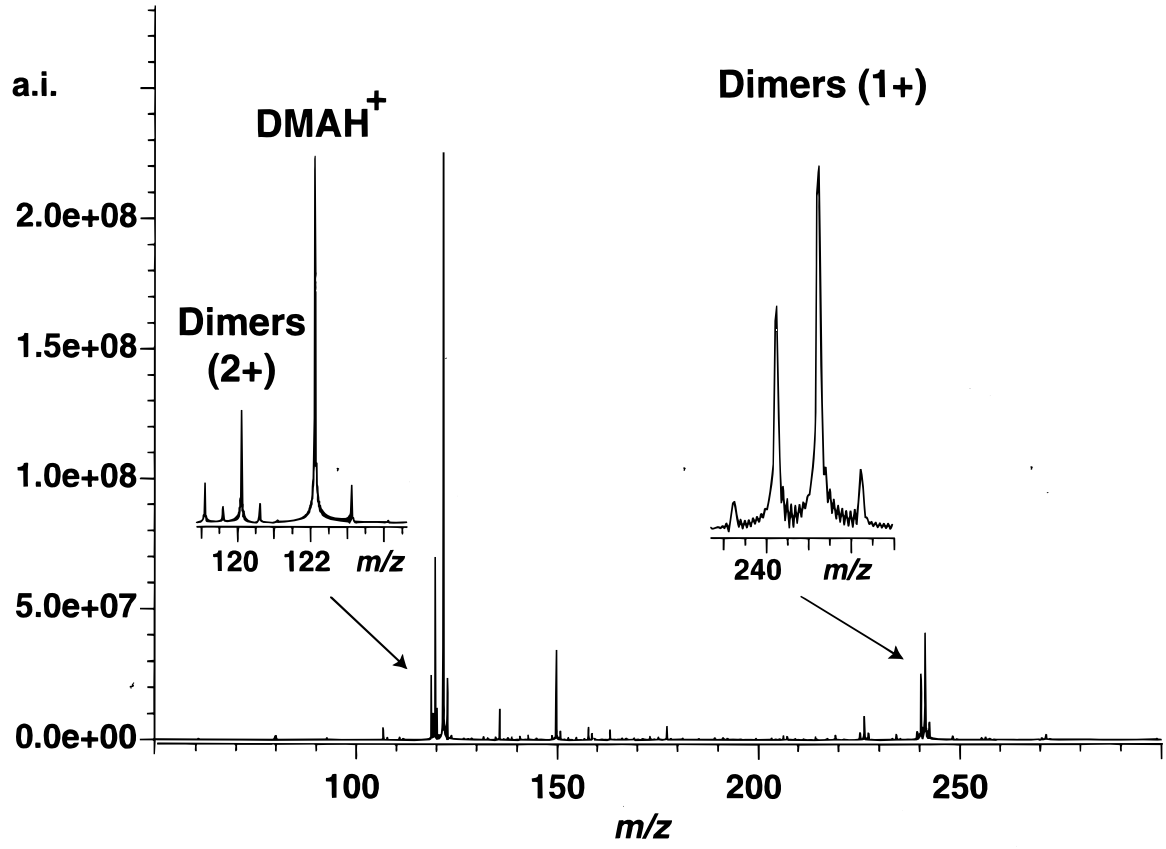

Figure 1. Spectrum of 30 μM DMA acquired by external source ESI-FTMS. Sum of 10 scans.

evident at *m/z* 122. The peaks at *m/z* 239, 240 and 241 correspond to singly charged dimeric products of DMA whose structures are elucidated here by MS/MS (see below). The peaks at *m/z* 119.1, 119.6 and 120.1 correspond to doubly charged dimer products whose structures were also elucidated by MS/MS (see below). Table 1 contains data from the MS/MS experiments on singly and doubly charged dimer products. An ' × ' entry in the table corresponds to the tabulated fragment ion appearing in the dimer species' tandem mass spectrum.

MS/MS experiments

The product ion tandem mass spectrum (using SORI-CAD) and fragmentation pathway of the *m/z* 241 dimer are illustrated in Fig. 2 and Scheme 1, respectively (the MS/MS fragmentation pattern remained the same independent of the hexapole accumulation time). The *m/z* values of the observed product ions are listed in Table 1. The *m/z* 226, 211, 196 and 181 peaks observed in Fig. 2 occur from consecutive losses of CH_3 groups. The *m/z* 167 peak corresponds to the loss of four CH_3s and the terminal nitrogen. The peak at *m/z* 77 corresponds to the phenyl radical cation and *m/z* 51 occurs from loss of neutral acetylene from this to form $[C_4H_3^{+\bullet}]$. The *m/z* 167 and 77 product ions clearly distinguish the dimerized product at *m/z* 241 as the proposed head-to-tail structure in Scheme 1. TMB (tail-to-tail dimer) is ruled out as a possible structure because the *m/z* 167 and 77 fragments cannot be generated from such a linkage. The only way an *m/z* 167 product ion can be formed from the dimer is through linkage of two aromatic rings by a nitrogen atom where the second ring has completely lost its dimethylaniline functionality (77 + 14 + 76 = 167 u). Also, SORI-CAD of the *m/z* 226 fragment ion (produced by dissociation in the ESI

Table 1. Fragment ions from MS/MS of DMA dimers[a]

Product ions observed (*m/z*)[b]	241 (+1)	240 (+1)	239 (+1)	120 (+2)	119.6 (+2)	119.1 (+2)
226	×	–	–	–	–	–
211	×	–	–	–	–	–
196	×	–	–	–	–	–
181	×	–	–	–	–	–
167	×	–	–	–	–	–
106	×	–	–	–	–	–
77	×	–	–	–	–	–
51	×	–	–	–	–	–
225	–	×	–	–	–	–
198	–	×	–	–	–	–
183	–	×	×	–	–	–
182	–	×	–	–	–	–
152	–	×	×	×	×	×
224	–	–	×	–	–	–
223	–	–	×	–	–	–
208	–	–	×	–	–	–
180	–	–	×	–	–	–
118	–	–	–	×	×	×
119.1 (+2)	–	–	–	×	×	–
119.6 (+2)	–	–	–	×	–	–

[a] ×, Fragment ion appears in the tandem mass spectrum; –, fragment ion does not appear in the tandem mass spectrum.
[b] +1 charge state except where shown as (2).

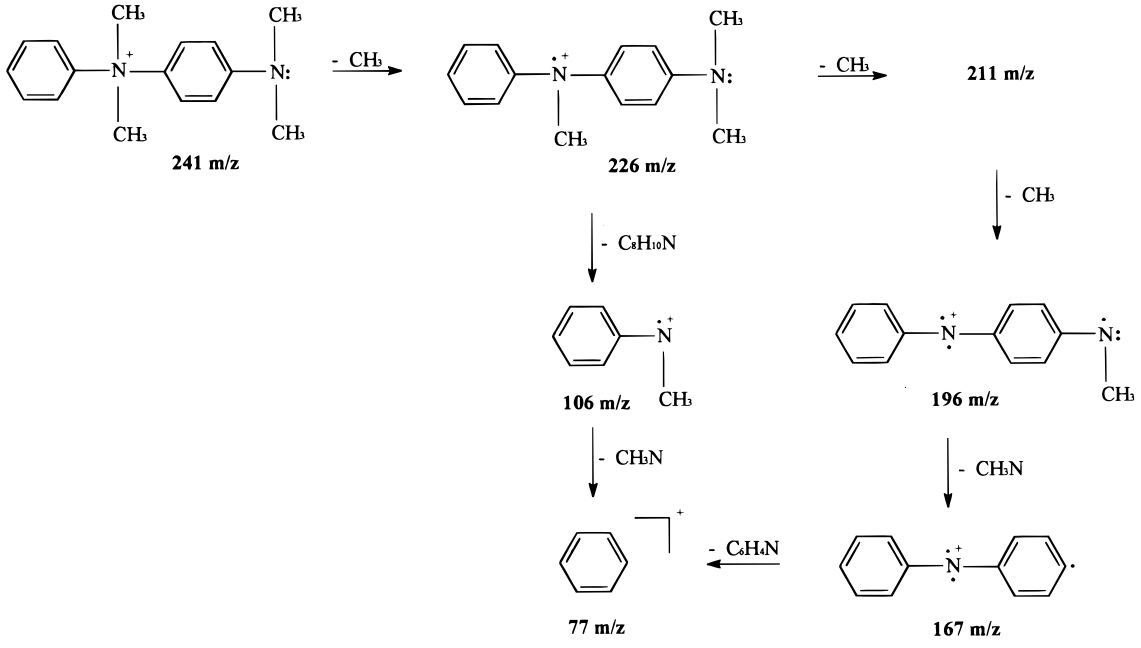

Scheme 1.

source) generates the *m/z* 167 product ion (data not shown), further supporting the fragmentation mechanism shown in Scheme 1. In addition, if the linkage is tail-to-tail, *m/z* 77 cannot be generated since the phenyl rings would have to be disubstituted. Additional evidence in support of the proposed dimeric structure in Scheme 1 comes from the *m/z* 196 product ion. The *m/z* 196 ion can be generated by the loss of $(CH_3)_2NH$ from $TMBH^+$ (with charge transfer back to the phenyl ring) or by loss of four CH_3s from the proposed structure in Scheme 1. An exact mass calculation determined the *m/z* 196 peak to correspond to the loss of four CH_3s, therefore disqualifying it as a possible fragment of $TMBH^+$.

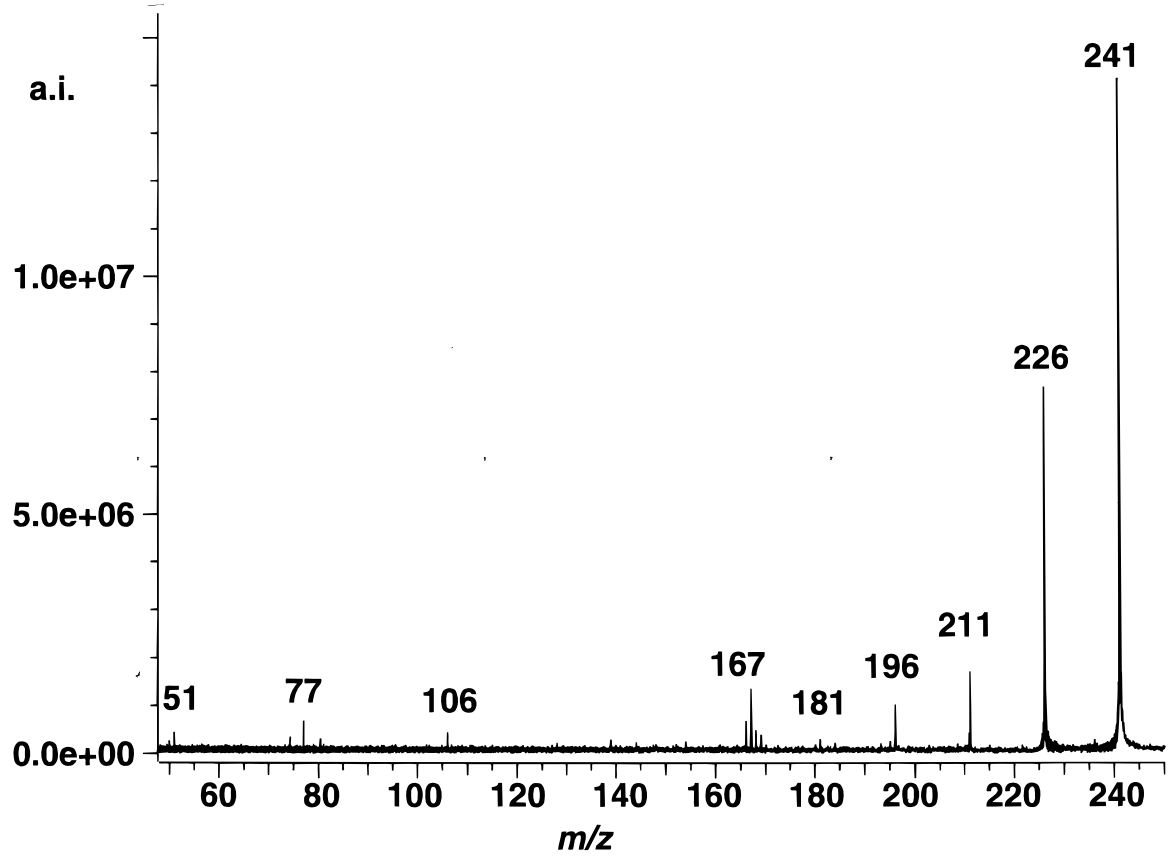

Figure 2. Tandem mass spectrum of *m/z* 241 DMA dimer by SORI-CAD using argon collision gas. An ion activation pulse of 0.3 s (~4 V_{pp}) with a frequency offset of −600 Hz was employed.

Using electrochemical thermospray MS, Hambitzer and Heitbaum[17] observed the *m/z* 241 ion from DMA and proposed that the species was $[TMBH]^+$, a tail-to-tail product. MS/MS was not used to confirm this assignment. The MS/MS pattern observed for the *m/z* 241 ion in our studies is only consistent with head-to-tail coupling, ruling out $TMBH^+$ as a possible structure. To our knowledge, the DMA dimer structure proposed in Scheme 1 has not been reported elsewhere. The detailed mechanism for how this product is formed in solution is not known, but it is probably the product of coupling amino protonated DMA ($[DMAH]^+$) with neutral DMA. The dimethylamino group on neutral DMA is a very strong electron donor that can activate the aromatic ring for *ortho–para* substitution.[14] The electron-donating strength of this substituent is responsible for making DMA susceptible to attack by weak electrophiles.[23] Nitrogen electrophiles have been studied extensively and are an integral component for nitrosation, nitration, diazonium coupling and amination reactions. Specifically, aryl azides can react with trifluoroacetic acid to generate the $ArNH^+$ electrophile, which can then react with an aromatic ring to form a diarylamine.[22,23] Similarly, we propose that the quaternary nitrogen in $[DMAH]^+$ acts as an electrophile and is responsible for the formation of the proposed structure in Scheme 1. Electrophilic aromatic substitution reactions of varying electrophiles and substituents are governed by a similar mechanism. In the first step, the π-electron system and electrophile form a donor–acceptor-type complex. In the second step, the intermediate sigma (σ) complex is formed in which the aromatic system is transformed into a cyclohexadienyl cation. The carbon, at the site of substitution, is bonded to both the electrophile and its substituent. The last step involves elimination of the substituent at the site of substitution (i.e. deprotonation).[23] In contrast to classical electrophilic aromatic substitution reactions, this coupling is unique in that it results in a moiety where the positive charge is retained at the nitrogen atom. The location of this charge is similar to what is found in ionene polymers, where positively charged atoms are located in the polymeric backbone.[29–31]

A 30 μM sample of diphenylamine was analyzed under the same experimental conditions (not shown). The protonated species occurred at *m/z* 170 with high abundance. The positively charged nitrogen in diphenylamine is formed within a similar environment (between two phenyl rings) as that proposed for the dimer product at *m/z* 241. This supports the idea that the quaternary ammonium form of nitrogen is stable in this acidic medium and can exist under the applied experimental conditions.

The SORI-CAD tandem mass spectrum and fragmentation scheme for the *m/z* 240 dimer are illustrated in Fig. 3 and Scheme 2, respectively. The *m/z* values of the observed product ions are listed in Table 1. The data suggests a tail-to-tail coupling product. A proposed structure for the *m/z* 240 dimer is TMB, as illustrated in Scheme 2 (see MS/MS evidence to support this structure below). The predominant mechanism of the ES ionization source is to assist in desolvating preformed ions in solution. However, Kebarle and co-workers[32,33] and Van Berkel and co-workers[34,35] have

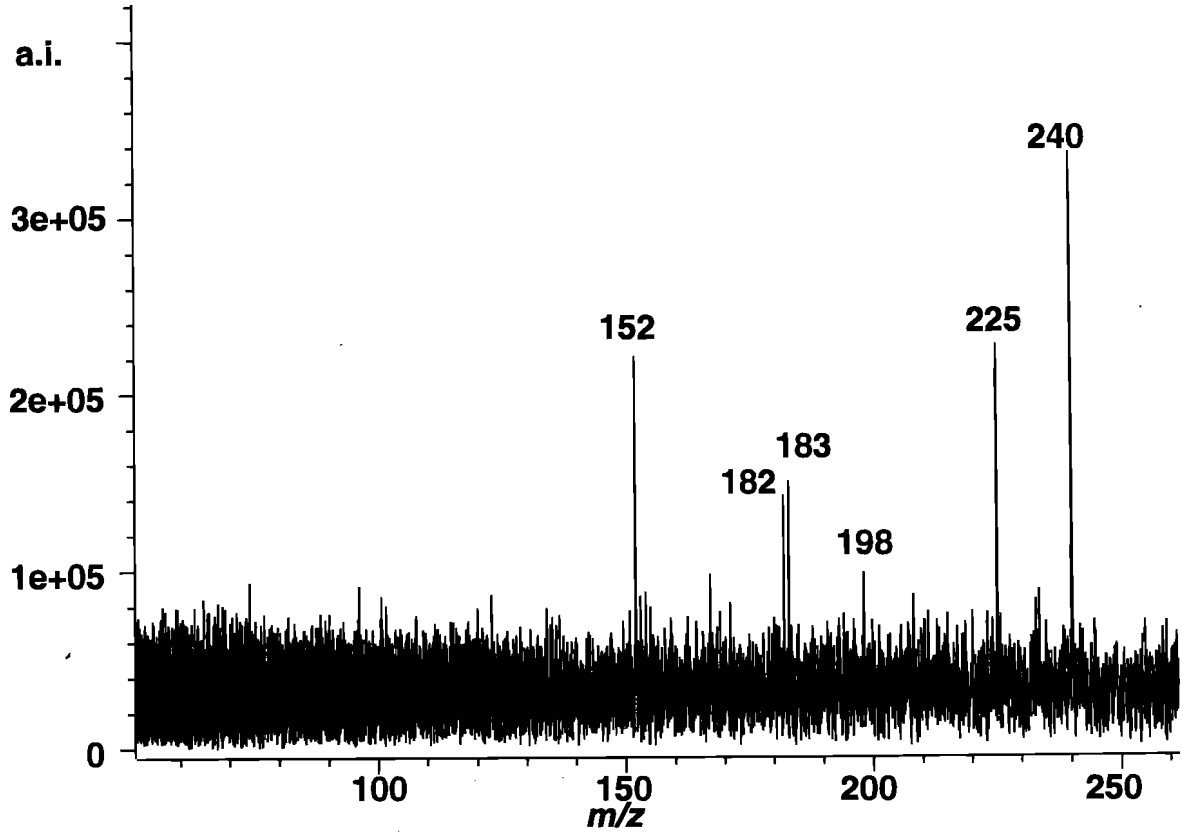

Figure 3. Tandem mass spectrum of *m/z* 240 DMA dimer by SORI-CAD using argon collision gas. An ion activation pulse of 0.5 s at an amplitude of ~1.6 V_{pp} and a frequency offset of −100 Hz was employed.

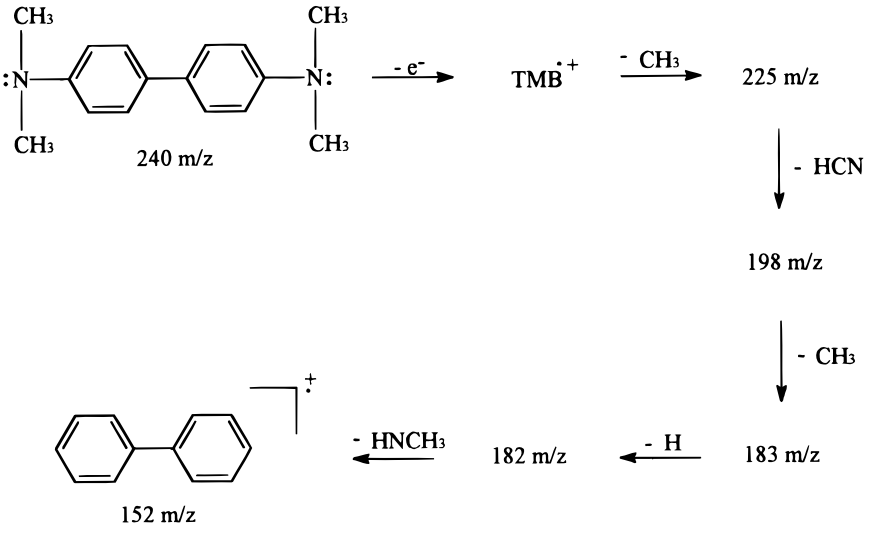

Scheme 2.

both independently demonstrated its inherent ability to act as an electrolytic cell due to charge balance requirements imposed by continual formation of charged droplets. Rapid and irreversible formation of TMB is known to occur when under the influence of an anodic potential.[13–16] A possible explanation for the formation of the proposed structure in Scheme 2 begins with oxidation of DMA at the metal/solution interface of the ES capillary to produce odd-electron radical cations. These radical cations could then couple, losing two protons in the process to form neutral TMB, which itself could be oxidized at the metal/solution interface to form $TMB^{+\cdot}$.

The MS/MS evidence supports TMB as the *m/z* 240 dimer, as shown in Scheme 2. First, $[TMB]^{+\cdot}$ loses a methyl radical to form the product ion at *m/z* 225, followed by neutral loss of HCN to form an *m/z* 198 fragment ion. The *m/z* 183 fragment ion can be produced by the loss of two methyls and HCN from the precursor; additional loss of a hydrogen leads to a fragment of *m/z* 182, as shown in Scheme 2. The fragment peak at *m/z* 152 suggests strongly that the dimer linkage is between two aromatic rings (tail-to-tail).

The SORI-CAD spectrum and fragmentation pathway of the *m/z* 239 dimer are illustrated in Fig. 4

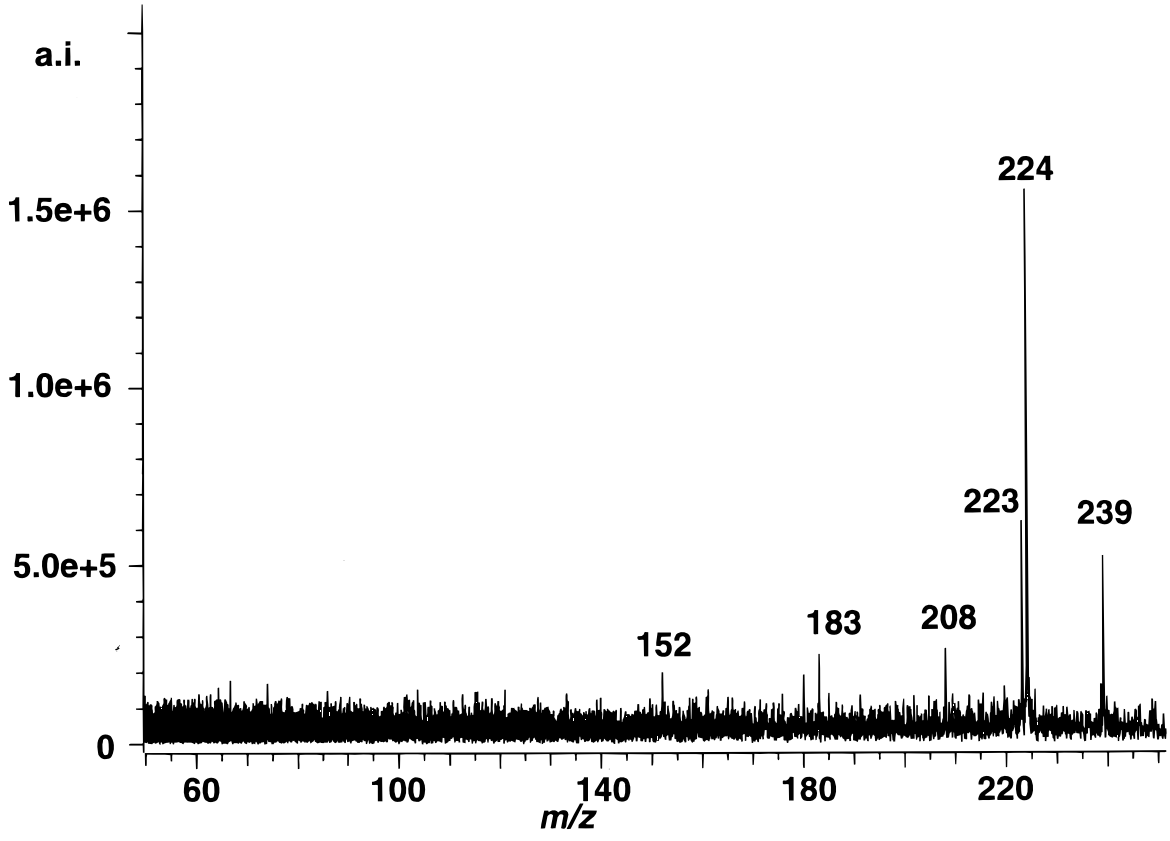

Figure 4. Tandem mass spectrum of *m/z* 239 DMA dimer by SORI-CAD using argon collision gas. An activation pulse of 0.3 s ($\sim$2 V_{pp}) with a frequency offset of −200 Hz was employed.

and Scheme 3, respectively. The *m/z* values of the products formed are listed in Table 1. The *m/z* 239 dimer is likely to be $[TMB^{2+} - H^+]^+$. The *m/z* 224 fragment ion is due to loss of a methyl group, followed by loss of a hydrogen atom to form *m/z* 223. The loss of a methyl group from *m/z* 223 produces the *m/z* 208 fragment, the proposed structure of which is shown in Scheme 3. Two consecutive losses of 28 u from *m/z* 208 (to *m/z* 180 and to *m/z* 152) reveals two NCH_2 units on opposing ends (Scheme 3). Again, the *m/z* 152 product ion is indicative of tail-to-tail linkage.

SORI-CAD tandem mass spectra of the (+2) dimer products are illustrated in Fig. 5(a)–(c) and the product ion *m/z* values are listed in Table 1. The mechanisms for the formation of these products are not known. The *m/z* 152 fragment peak appears in all the spectra, and suggests tail-to-tail coupling products. The *m/z* 119.6 (+2) and 119.1 (+2) dimers are product ions from the fragmentation of the *m/z* 120.1 (+2) dimer. The *m/z* 119.1 (+2) dimer is also a product ion from the fragmentation of the *m/z* 119.6 (+2) dimer. In addition, all tandem mass spectra of (+2) dimers produce an *m/z* 118 product ion corresponding to $[C_8H_8N]^+$. The similarities in the fragmentation patterns for the mass spectra illustrated in Fig. 5(a)–(c) are probably due to the close similarities in structure of these doubly charged dimers.

We propose that the formation of the *m/z* 119.1 (+2), 119.6 (+2) and 120.1 (+2) dimers occurs from oxidation of either neutral or singly charged TMB. A proposed scheme for the formation of the dimers is illustrated in Scheme 4. After oxidation to doubly charged TMB, a proton can be lost to form $[TMB^{2+} - H^+]^+$ (*m/z* 239, see Scheme 3). This species may be further oxidized to form $[TMB^{2+} - H^+]^{2+}$.

Figure 6 presents data from a 30 μM DMA sample and illustrates the relative ion abundance of monomeric and dimeric products as the capillary voltage is

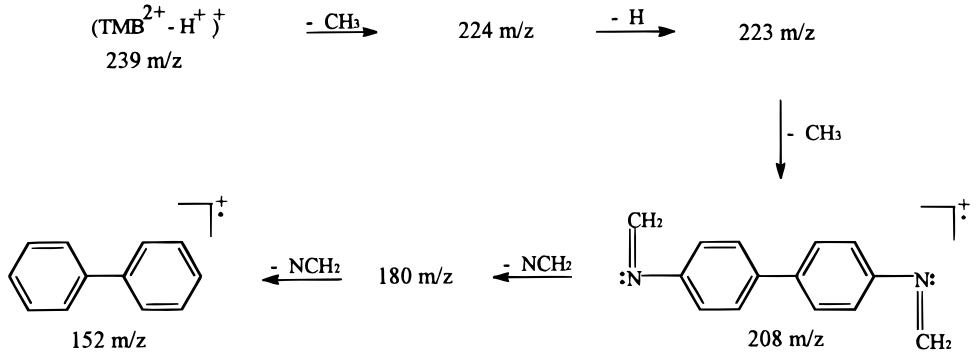

Scheme 3.

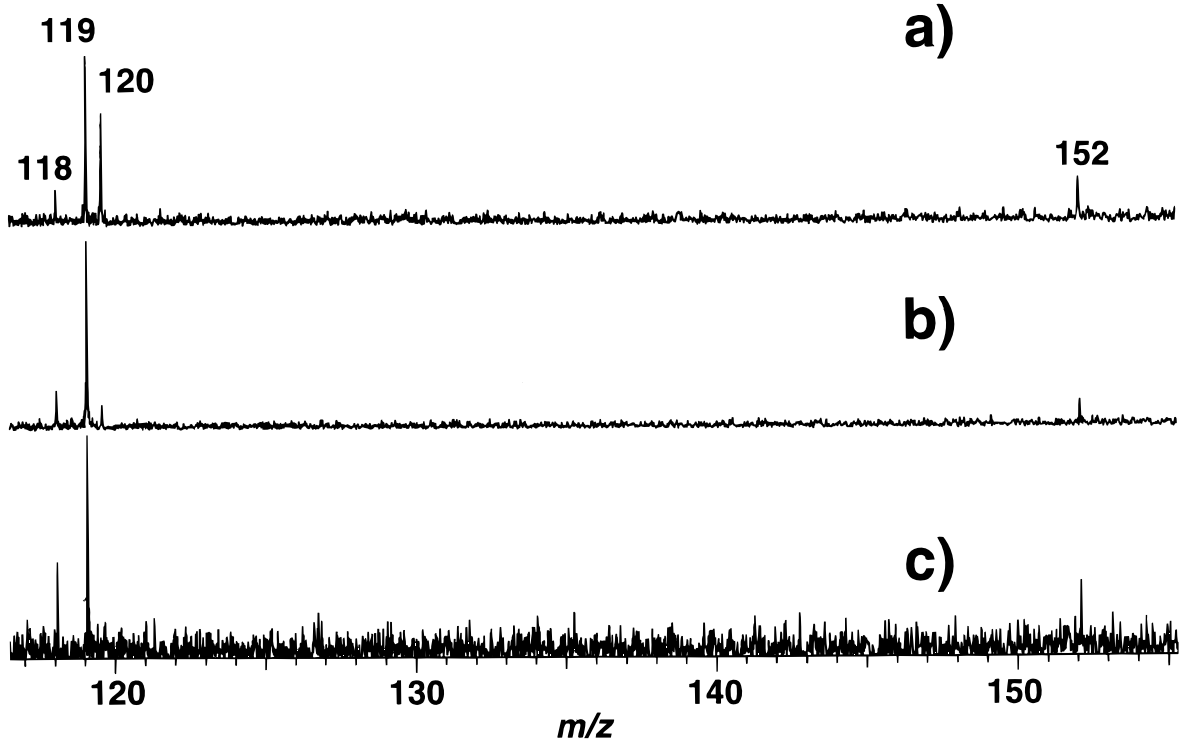

Figure 5. Tandem mass spectra of +2 DMA dimers; (A) *m/z* 119.1, (B) *m/z* 119.6 and (C) *m/z* 120.1. Proceeding from top to bottom, the SORI-CAD r.f. activation conditions were (A) 0.3 s pulse, ~1.5 V_{pp}, −200 Hz off-resonance, (B) 0.3 s pulse, ~1.8 V_{pp}, −400 Hz off-resonance and (C) 0.5 s pulse, ~1.2 V_{pp}, −100 Hz off-resonance.

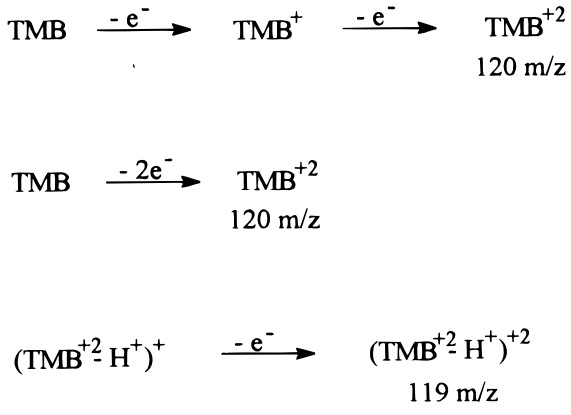

Scheme 4.

increased. A steady decrease in monomeric $[DMAH]^+$ is apparent. The *m/z* 120.1 and 119.6 dimers increase in abundance initially and then decrease while the *m/z* 119.1 dimer steadily increases in abundance. This supports the idea that oxidation at the metal surface of the capillary or skimmer may be the source of production of these dimers. The eventual decrease of the *m/z* 119.6 and 120.1 dimers probably occurs from nozzle–skimmer dissociation, resulting in the loss of one and two hydrogen atoms, respectively, to form the *m/z* 119.1 dimer product.

Hexapole ion accumulation study

Several interfaces for coupling ES ionization and FTMS have been developed.[36–41] Our commercial FTMS contains an r.f. only hexapole, which serves to store and accumulate ions immediately following the ES ionization source. Ions can be stored in the hexapole for up to 30 s before introduction into the electrostatic ion optic channel used to guide ions to the FTMS ion trap. By accumulating precursor ions in the hexapole for

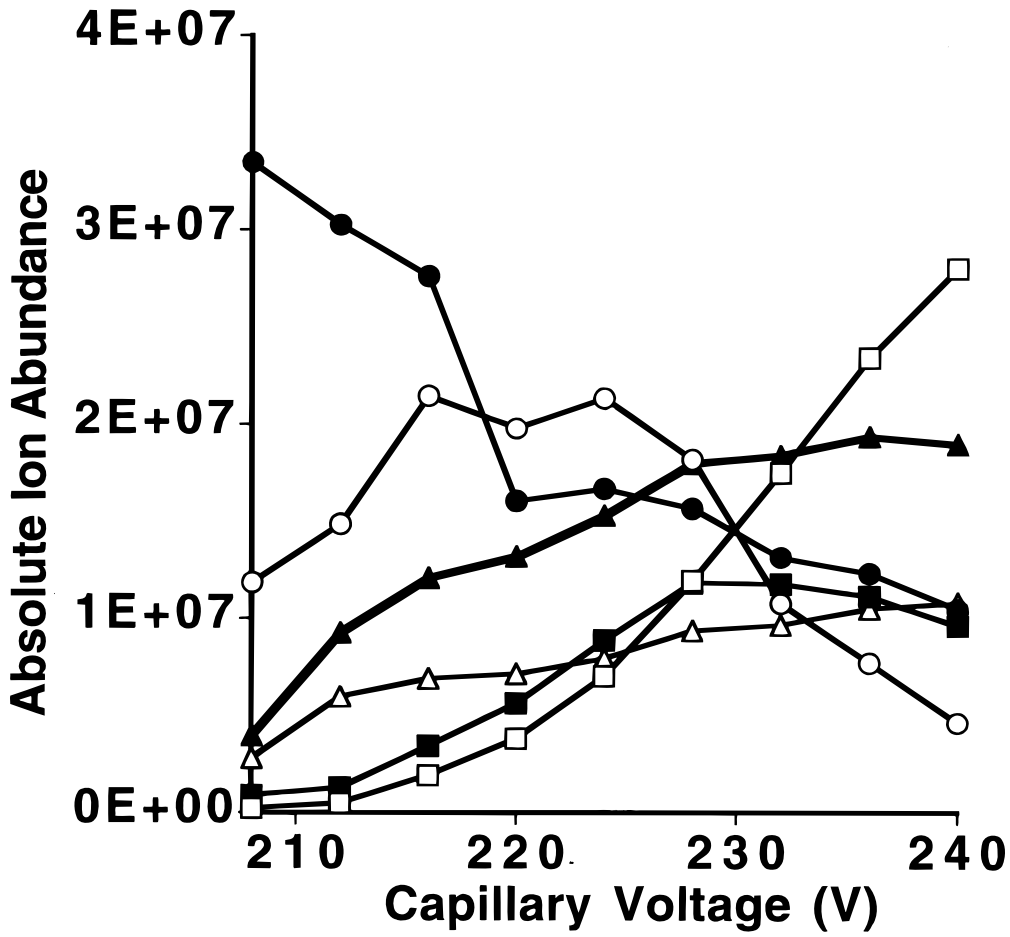

Figure 6. Relative ion abundance, for a 30 μM sample of DMA, of monomer (●, *m/z* 122) and dimeric products (□, *m/z* 119.1 (+2); ■, *m/z* 119.6 (+2); ○, *m/z* 120.1 (+2); △, *m/z* 239 (+1); ▲, *m/z* 240 (+1)) as a function of applied capillary voltage (skimmer held constant at 47 V).

extended trapping times, it is possible to increase greatly the ion abundances detected in the FTMS trap. This is especially valuable when an ESI-generated ion is of low abundance initially without accumulation; with accumulation, its population significantly increases such that MS/MS of the ion becomes practical. Indeed, for most applications where the precursor ion does not react with its neutral form or other molecular species which may be present in the ESI solvent system (e.g. non-volatile species), hexapole accumulation of precursor ions is fairly successful. It should be noted that ion accumulation will not occur if the precursor ion reacts with neutrals in the molecular beam generated by ESI. In such cases. ion–molecule reactions will occur, and the precursor ion's abundance may actually *decrease* while stored in the hexapole, rather than increase. Figure 7 contains data from a 30 μM DMA sample, illustrating the relative ion abundances of monomer and dimers as the ion storage time is increased from 1 to 10 s. Interestingly, the relative abundance of dimeric species increases while the monomer decreases in abundance with increased ion storage time. Clearly $[DMAH]^+$ formed in the ESI solution is reacting with neutral DMA in the molecular beam from the ESI source to form the dimeric ion–molecule reaction products. Dimerization of DMA appears to be relatively facile in the gas phase *vs.* the liquid phase. One potential application of this phenomenon could be for conducting ion–molecule reactions at high pressure via introduction of a reagent gas into this region. This would be useful for conducting slow ion–molecule reactions or to keep the reagent gas from the high-vacuum region where the ion trap is housed and where high pressure is detrimental to optimal FTMS detection. An external hexapole/internal trap is analogous to the dual-trap arrangement[42] which has shown high utility for conducting ion–molecule reactions at high pressure with subsequent transfer of products to a low-pressure trap for optimal FTMS detection.[43]

CONCLUSION

ESI-FTMS shows that DMA forms a variety of dimeric products when in acidic solution. MS/MS of these different dimers shows that most dimeric species have tail-

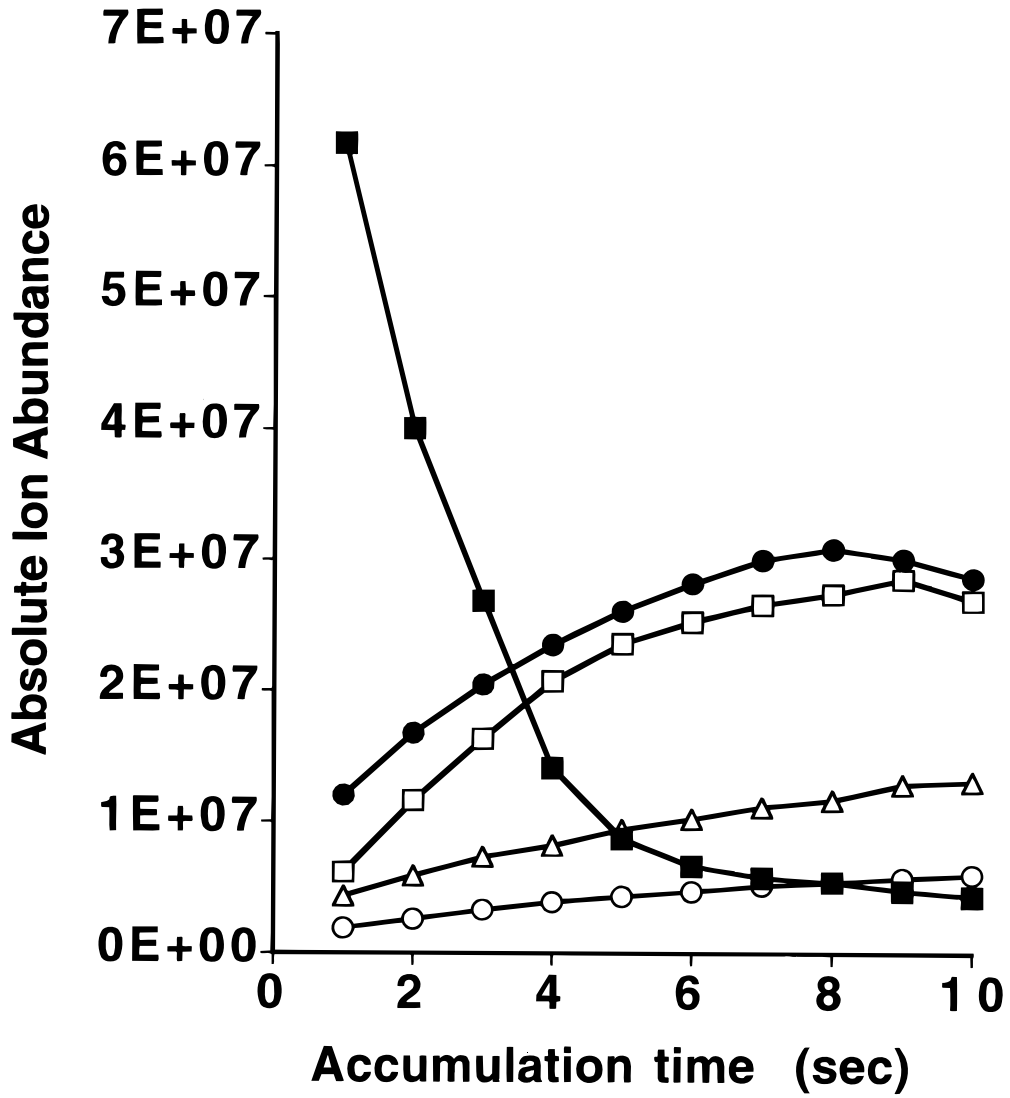

Figure 7. Plot of relative ion abundance, for a 30 μM sample of DMA, of monomer (■, *m/z* 122) and dimeric ions (□, *m/z* 120 (+2); ○, *m/z* 239 (+1); △, *m/z* 240 (+1); ●, *m/z* 241 (+1)) as a function of storage time (1–10 s) in the hexapole ion guide.

to-tail linkages such as TMB and other closely related structures which are known to be produced by anodic oxidation of DMA. However, a dimeric species with head-to-tail linkage is also observed, presumably via coupling of $[DMAH]^+$ to the *para* position of neutral DMA. In addition, there is strong evidence for ion–molecule reactions occurring within the hexapole storage region of the ESI source. This suggests that reagent gas may be purposefully introduced into this region through an injection port to facilitate ion–molecule reactions between it and the electrosprayed analyte ions at high pressure, away from the ion trap in the high-vacuum region of the FTMS system.

Acknowledgements

We thank Sarah Lorenz, Hank Padley, Sajid Bashir, Xuling Gao, Craig Dufresne, Gary Baker and Mike Cieslak for helpful suggestions. Acknowledgement is made to the donors of the Petroleum Research Fund, administered by the American Chemical Society, and the State University of New York at Buffalo for support of this research.

REFERENCES

1. T. Sato, M. Takada and T. Otsu, *Makromol. Chem.* **148**, 239 (1971).
2. S. Lenka, P. L. Nayak and A. Basak, *J. Polym. Sci. Chem. Part A* **24**, 3139 (1986).
3. P. Ghosh and D. K. Chowdhury, *J. Polym. Sci. Chem. Part A* **23**, 1407 (1985).
4. N. Oyama, T. Ohsaka and T. Shimizu, *Anal. Chem.* **57**, 1526 (1985).
5. L. R. Sharma, A. K. Manchandra, G. Singh and R. S. Verma, *Electrochim. Acta* **27**, 223 (1982).
6. N. L. Weinber and T. B. Reddy, *J. Am. Chem. Soc.* **90**, 91 (1968).
7. E. T. Seo, R. F. Nelson, J. M. Fritsch, L. S. Marcoux, D. W. Leedy and R. N. Adams, *J. Am. Chem. Soc.* **88**, 3498 (1966).
8. R. L. Hand and R. F. Nelson, *J. Am. Chem. Soc.* **96**, 850 (1974).
9. D. M. Mohilner, R. N. Adams and W. J. Argersinger, Jr, *J. Am. Chem. Soc.* **84**, 3618 (1962).
10. J. McMurray, *Organic Chemistry*, 3rd edn. Brooks/Cole, Belmont, CA (1992).
11. A. Volkov, G. Tourillon, P. Lacaze and J. Dubois, *J. Electroanal. Chem.* **155**, 279 (1980).
12. W. W. Focke and G. E. Wnek, in *Proceedings of an American Chemical Society Symposium on Electroactive Polymers, Denver, CO, April 6–10, 1987*. American Chemical Society, Washington DC (1987).
13. T. Mizoguchi and R. N. Adams, *J. Am. Chem. Soc.* **84**, 2058 (1962).
14. Z. Galus, R. M. White, F. S. Rowland and R. N. Adams, *J. Am. Chem. Soc.* **84**, 2065 (1962).
15. Z. Galus and R. N. Adams, *J. Am. Chem. Soc.* **84**, 2061 (1962).
16. G. Neubert and K. B. Prater, *J. Electrochem. Soc.* **121**, 745 (1974).
17. G. Hambitzer and J. Heitbaum, *Anal. Chem.* **58**, 1067 (1986).
18. F. W. McLafferty (Ed.), *Tandem Mass Spectrometry*. Wiley, New York (1983).
19. K. L. Busch, G. L. Glish and S. A. McLuckey, *Mass Spectrometry*/Mass Spectrometry: Techniques and Applications of Tandem Mass Spectrometry. VCH, New York (1988).
20. J. B. Fenn, M. Mann, C. K. Meng, S. F. Wong and C. M. Whitehouse, *Science* **246**, 64 (1989).
21. G. J. Van Berkel, S. A. McLuckey and G. L. Glish, *Anal. Chem.* **63**, 2064 (1991).
22. R. Taylor, *Electrophilic Aromatic Substitution*. Wiley, New York (1990).
23. F. A. Carey and R. J. Sundberg, *Advanced Organic Chemistry*, 3rd edn. Plenum Press, New York (1990).
24. P. Caravatti and M. Allemann, *Org. Mass Spectrom.* **26**, 514 (1991).
25. R. L. C. Lau, J. Jiang, D. K. P. Ng and T.-W. D. Chan, *J. Am. Soc. Mass Spectrom.* **8**, 161 (1997).
26. H. R. Padley, S. Bashir and T. D. Wood, *Anal. Chem.* **69**, 2914 (1997).
27. P. Caravatti, *US Pat.* 4 924 089 (1990).
28. J. W. Gauthier, T. R. Trautman and D. B. Jacobson, *Anal. Chim. Acta* **246**, 211 (1991).
29. A. Rembaum, *J. Macromol. Sci. Chem.* **A3**, 87 (1969).
30. D. Casson and A. Rembaum, *Macromolecules* **5**, 75 (1972).
31. A. Rembaum and H. Noguchi, *Macromolecules* **5**, 261 (1972).
32. A. T. Blades, M. G. Ikonomou and P. Kebarle, *Anal. Chem.* **63**, 2109 (1991).
33. M. G. Ikonomou, A. T. Blades and P. Kebarle, *Anal. Chem.* **63**, 1989 (1991).
34. G. J. Van Berkel, S. A. McLuckey and G. L. Glish, *Anal. Chem.* **64**, 1586 (1992).
35. G. J. Van Berkel and F. Zhou, *Anal. Chem.* **67**, 2916 (1995).
36. L. Tang, R. L. Hettich, G. B. Hurst and M. V. Buchanan, *Rapid Commun. Mass Spectrom.* **9**, 731 (1995).
37. C. B. Lebrilla, I. J. Amster and R. T. McIver, Jr, *Int. J. Mass Spectrom. Ion Processes* **87**, R 7 (1989).
38. M. T. Rodgers, S. Campbell, E. M. Marzluff and J. L. Beauchamp, *Int. J. Mass Spectrom. Ion Processes* **137**, 121 (1994).
39. P. A. Limbach, A. G. Marshall and M. Wang, *Int. J. Mass Spectrom. Ion Processes* **125**, 135 (1993).
40. S. C. Beu, M. W. Senko, J. P. Quinn, F. M. Wampler, III, and F. W. McLafferty, *J. Am. Soc. Mass Spectrom.* **4**, 557 (1993).
41. B. E. Winger, S. A. Hofstadler, J. E. Bruce, H. R. Volseth and R. D. Smith, *J. Am. Soc. Mass Spectrom.* **4**, 566 (1993).
42. D. P. Littlejohn and S. Ghaderi, *US Pat.* 4 581 533 (1986).
43. K. M. Stirk, M. Kiminkinen and H. I. Kenttämaa, *Chem. Rev.* **92**, 1649 (1992).